



Royal Netherlands Institute for Sea Research

This is a postprint of:

Witbaard, R.; Bergman, M.J.N.; van Weerlee, E.M. & Duineveld, G.C.A. (2017). An estimation of the effects of *Ensis directus* on the transport and burial of silt in the near-shore Dutch coastal zone of the North Sea. *Journal of Sea Research*, 127, 95-104

Published version: <https://dx.doi.org/10.1016/j.seares.2016.12.001>

Link NIOZ Repository: www.vliz.be/nl/imis?module=ref&refid=282995

[Article begins on next page]

The NIOZ Repository gives free access to the digital collection of the work of the Royal Netherlands Institute for Sea Research. This archive is managed according to the principles of the [Open Access Movement](#), and the [Open Archive Initiative](#). Each publication should be cited to its original source - please use the reference as presented.

When using parts of, or whole publications in your own work, permission from the author(s) or copyright holder(s) is always needed.

1 An estimation of the effects of *Ensis directus* on the transport
2 and burial of silt in the near-shore Dutch coastal zone of the
3 North Sea

4

5 Rob Witbaard*^a, Magda J.N. Bergman^a, Evaline van Weerlee^a, Gerard C.A. Duineveld^a

6

7 a: Royal Netherlands Institute for Sea Research (NIOZ) and Utrecht University, P.O. Box 59, 1790 AB
8 Den Burg, the Netherlands.

9

10

11 *Corresponding author. Tel: +31222369537.

12

13 E-mail addresses: Rob.Witbaard@nioz.nl

14 Gerard.Duineveld@nioz.nl

15 Magda.Bergman@nioz.nl

16 Evaline.van.Weerlee@nioz.nl

17

18

19

20 **ABSTRACT**

21 This paper describes the distribution of the razor clam *Ensis directus* in the Dutch coastal zone
22 with emphasis on its relation to sediment grainsize, in particular silt. The study includes a spatial
23 survey along the coast of North Holland (Netherlands) and an in-situ experiment for the burial of silt.
24 Densities of *E. directus* appeared highest close to the coast in the siltiest sediment, where also the
25 highest body mass index values (BMI) were found suggesting the best conditions for growth. The
26 largest specimens with the lowest BMI were found at the less silty, outermost off-shore stations.

27 In the shallow (10 m) zone a "lander" frame was deployed at the seabed containing ~100 pvc
28 tubes filled with silt free sand that each hosted either a living *E. directus*, an empty shell, or bare
29 sand. After three 3-weeks periods the silt content in the different tubes was determined and
30 compared. The silt content around a living *E. directus* appeared 34% (spring) and 12% (autumn)
31 higher than around an empty vertical shell, and 56% (spring) higher than in bare sand.

32 We discuss the different pathways along which silt is brought into subsurface sediment layers
33 and speculate about the potential role of *E. directus* in the coastal sediment and silt dynamics. It is
34 estimated that *E. directus* facilitates the (temporal) burial of up to 6 Mton of fine particles in the
35 coastal zone annually. This equals up to 27% of the annual SPM transport along the Dutch coast and
36 is between 45 and 85% of the annual influx into the western Wadden Sea.

37 The results show that the coastal *E. directus* population has a large impact on mass balance
38 and behaviour of SPM, and on the ecological functioning of Dutch coastal and estuarine ecosystems.

39
40

41 **Keywords:**

42 North Sea

43 *Ensis directus*

44 Silt burial

45 Beach nourishment

46 Ecological Impact

47

48 1. INTRODUCTION

49 Presently the American razor clam *Ensis directus* is the most abundant bivalve species along the
50 Dutch coast. This species which originates from the US east coast has rapidly spread along north
51 western European coasts since it was first observed in the German Bight in 1979 (Von Cosel *et al.*,
52 1982; Armonies, 2001; Severijns, 2002), and from where it migrated to other areas (Arias & Anadón,
53 2012, Severijns, 2002, Dauvin *et al.*, 2007). *E. directus* prefers to live in dynamic sedimentary
54 conditions mostly in mobile sands where it can rapidly retract itself deep into the sediment (Drew
55 1907; Trueman, 1967). Annual surveys by Goudswaard *et al.* (2013) showed that this species is
56 presently dominating the macrobenthic biomass in the Dutch coastal zone and that its local standing
57 stock is substantially higher than estimates of total bivalve biomass prior to its appearance. There is
58 some debate whether this newcomer outcompeted native species. Dannheim & Rumohr (2012)
59 supposed that that was not the case because its preferred habitat of mobile sands with high current
60 speeds (Dekker & Beukema, 2012) has never been fully occupied by native bivalves. Severijns (2002)
61 furthermore argues that it is very unlikely that *E. directus* has outcompeted other *Ensis* species, since
62 historical records suggest that latter were not very common along our coast. The other species were
63 still found along the beaches even 10 years after *E. directus* had invaded Belgian waters.

64 Since *E. directus* invaded European waters it has become an ecologically important species in
65 coastal waters. Fish and birds have started feeding on it (Tulp *et al.*, 2010; Cadee, 2000; Wolf &
66 Meininger, 2004) and densities have become so high that a commercial *Ensis* fishery has developed.
67 Dense beds might support a higher diversity of associated macrofauna in response to associated
68 changes in the silt and organic content (Armonies & Reise, 1999). Near the island of Sylt they found
69 an increase of the silt and organic content in a dense *E. directus* bed which they ascribed to the local
70 production of fine faecal material. Though winter storms removed this fine fraction from the
71 surface, it was retained in deeper sediment layers at their Sylt station. Given the massive numbers of
72 *E. directus* along the entire Dutch coast (Goudswaard *et al.*, 2013) a similar entrainment of silt could
73 possibly be a significant term in the budget of alongshore tidal transport of silt and other SPM (RIKZ,
74 2002). At the same time this stretch of coast is subject to erosion requiring continuous shoreface
75 and beach nourishments for maintenance. In the period 2013-2016 roughly 28×10^6 m³ sediment is
76 supplied on the North-Holland coast consisting mainly of sand with a small admixture of silt, which
77 adds to the turbid coastal "river" running north. If *E. directus* actively influences the burial of silt its
78 dense coastal population might have a significant influence on the transport budget of this fine
79 sediment fraction.

80 Quantitative data on the rate of silt entrainment by *E. directus* are lacking. This study aims to
81 assess this rate and explores *Ensis'* relationship with sediment grain size on a wider scale along the

82 coast of North-Holland. We experimentally tested whether living *E. directus* is capable of changing
83 the sedimentary characteristics of a sediment core under in-situ conditions in this shallow, dynamic
84 coastal zone, and compared the sedimentary impact of alive individuals with that of empty shells
85 and bare sand. The experiments were conducted in conjunction with a survey on spatial distributions
86 of this species and associated sedimentary conditions in the coastal zone of North-Holland.

87

88 2. Methods

89 2.1 Coastal distribution *Ensis directus*

90 In June 2011 a synoptic sampling survey was conducted covering a large part of the coastal zone of
91 North Holland. Median grain size is 222 μm with 5.1% silt. The area is characterised by a marked
92 seasonal cycle in bottom water temperature and primary production. At the end of summer the
93 highest temperature reaches 18°C. The salinity varies between 26 PSU in winter-spring and 32 PSU in
94 summer. Maximum current speeds vary over the neap-spring cycle between 70 and 120 cm s^{-1} . The
95 most near shore area is characterised by the existence of a turbidity maximum zone (TMZ) (van der
96 Hout *et al.*, 2015). More details about the area can be found in van der Hout *et al.* (2016; this
97 volume) and in Witbaard *et al.* (2015).

98 During the sampling campaign 12 boxcore samples were collected from each of 8 transects
99 perpendicularly oriented to the coast. Each transect extended up to 6 km from the coast and the 12
100 sampling stations had a depth profile from 8 to 19 meter. From each boxcore (diameter 30 cm) a 10
101 cm long, 35 mm diameter subcore was taken. This core was split in a 0-5 cm and a 5-10 cm layer
102 which were separately analysed for grainsize composition. The freeze dried sediment sample was
103 sieved over a 2 mm screen, homogenized and analysed on a Beckman Coulter LS 13 320. The size
104 range of particles that could be measured was 0.4-2000 μm which excludes clay particles (*i.e.*
105 particles < 0.4 μm). Hence the fraction 0.4-63 μm is accordingly denominated as “silt” (Wentworth
106 Class) in following paragraphs. Apart from freeze drying of the sediment samples, no other
107 treatments (oxidizing/acidification) were performed. Since none of such pre-treatments were
108 performed the particle size spectrum will not necessarily be similar to silt contents and grain size
109 composition as reported by geologists which do apply such methods. Notably our sediment data will
110 also be based on the organic material in the samples.

111 The rest of the boxcore content was sieved over a 1 mm screen and *E. directus* were sorted
112 out. Shell length, width and height were measured with digital callipers to the nearest 0.1 mm. Shell
113 width (thickness) and height were measured at the posterior side (siphon) of the shell. In case a shell
114 was collected incompletely (*i.e.* mostly only the siphon side) shell length was estimated from the
115 shell width and the relationship between shell width and length found for complete shells. The soft

116 body tissues were removed and dried until constant weight at 60°C. The weight of the dried bodies
117 was determined after which the organic parts were incinerated at 540 °C for 4 hours. The remaining
118 material (ash) was weighed. Ash Free Dry Weight (AFDW) was subsequently calculated as the
119 difference between dry weight and ash weight. AFDW and shell measurements were used to
120 calculate the body mass index (BMI) or condition. Condition expresses the tissue weight per
121 standard shell volume. Shell volume was calculated as shell length × shell height × shell width
122 instead of shell length³, since population data collected in 2011 and 2012 (Witbaard *et al.*, 2015)
123 showed that if length³ was used, the body condition remained dependent of shell length. Hence the
124 condition indices presented here differ from those reported by other authors like *e.g.* Dekker &
125 Beukema (2012). The calculated condition indices were used to depict spatial patterns in the body
126 condition, *i.e.* across and along shore. BMI and size (expressed as AFDW ind⁻¹) of *E. directus* in
127 combination with environmental data (grainsize, depth, distance) were used in a redundancy
128 analyses (R; Package Vegan; Oksanen *et al.*, 2013) to identify which environmental factor could
129 explain its distribution, size and condition in the study area.

130

131 **2.2 Silt burial experiment**

132 **2.2.1 Experimental setup**

133 In 2010 burial of silt by *E. directus* was investigated *in-situ* by deploying experimental trays mounted
134 on a measurement platform (“lander”) at a ~10 meter deep site off the coast of Egmond
135 (52°38.249'N 04°36.294'E, Fig 2; Witbaard *et al.*, 2015) within a dense *E. directus* population. The
136 lander consists of a triangular aluminium frame (height × width: 2 × 2 m) with a series of ballast
137 weights (total 500 kg) fixed onto its lowest horizontal structure. The platform was equipped with
138 three mesocosm trays (97*25*16 cm, with the top side 54 cm above seabed). During the
139 deployment periods each of the three mesocosms contained 36 PVC tubes with a diameter of 7 cm
140 and a length of 15 cm. Each tube was filled with well sorted sand with a median grain size of ~ 314
141 µm and an average silt content of 0.12 %. Within each mesocosm, three treatments, *i.e.* tubes with
142 three different types of fillings, were tested. Half of the tubes carried a living *E. directus* of
143 approximately 100 mm long. A quarter of the tubes contained an vertically positioned empty *E.*
144 *directus* shell of the same length and the other quarter of the tubes were filled with sand only. Just
145 before deployment of the lander the prepared tubes with the 3 different types of filling (treatments)
146 were regularly distributed within and between each of the 3 mesocosm trays. At the time of
147 deployment the mesocosms were closed with a hydraulically operated lid. The lid opened 1 hour
148 after deployment. At the end of the deployment period the hydraulic lids were closed again at a pre-

149 set date and time. The closure of the lids prevented wash out of sediments from the tubes during
 150 deployment and recovery of the measurement platform.

151 The lander furthermore carried a series of instruments to monitor biotic and abiotic
 152 conditions at heights between 30 cm and 200 cm above the bottom. The instrument package
 153 comprised a current meter (speed-direction-pressure), a CTD (temperature, salinity) and several
 154 turbidity and fluorescence sensors. Detailed information about these measurements is given in
 155 Witbaard *et al.* (2013, 2015) and Van der Hout *et al.* (submitted).

156 In 2010, the platform was successfully deployed 3 times for a 3-weeks period *i.e.* twice in
 157 spring 2010 and once in autumn 2010 (Table 1). After recovery of the measurement platform from
 158 the seabed, the depth of the sediment surface below the top edge of each tube was measured. For
 159 the analyses only tubes were used from which the sediment surface was at maximum 1cm below the
 160 top edge of the PVC tube. An a-priori selection of tubes was randomly made. In case a living *Ensis* in
 161 one of these selected tubes had died, the nearest tube with a living *Ensis* was selected. Tubes with a
 162 shell of which the animal had died during the deployment were not used. The specimen could have
 163 died shortly after the start of the deployment implying that the length over which the animal could
 164 have influenced silt distribution is unknown. The contents of the tubes were used in the grain size
 165 analyses following the procedure described in section 2.1.

166
 167 Table 1. Overview of deployment periods, start and end dates, and number of tubes per treatment that were analysed.
 168 Numbers in brackets indicate the total number of 1 cm sliced layers which were analysed. NB In autumn no tubes with only
 169 sand were analysed (-).
 170

Period	weeknr	Start dd/mm/yyyy	End dd/mm/yyyy	nr of days	nr tubes (nr layers) Empty shell	nr tubes (nr layers) Living <i>Ensis</i>	nr tubes (nr layers) Only sand
Spring 2010	wk 10-14	12/03/2010	06/04/2010	25	10 (139)	17 (237)	10 (139)
Spring 2010	wk 14-17	09/04/2010	26/04/2010	17	11 (123)	14 (160)	11 (120)
Autumn 2010	wk 41-44	13/10/2010	01/11/2010	19	12 (273)	15 (353)	-

171
 172

173 **2.2.2 Spring experiments**

174 In spring the lander was deployed during two periods (week 10-14 and week 14-17 (Table 1) of
 175 respectively 25 and 17 days. The contents of the tubes from the spring deployments (Table 1) were
 176 sliced in 1 cm slices down to 10 cm depth. Layers deeper than 10 cm were pooled and regarded as
 177 one sample. Each slice was labelled, frozen and subsequently freeze-dried. These freeze-dried

178 samples were used in the grain size determination (see section 2.1). The depth distribution of grain
179 size and silt content of the different treatments was statistically compared .

180 The statistical comparison was firstly done by comparing the treatments layer by layer with a
181 Kruskal-Wallis test to identify whether a difference in sediment silt content existed. To test which
182 factors contributed to the observed differences between treatments and over the full depth range of
183 the tubes, a generalized additive mixed model (GAMM; Wood, 2006) was fitted. In the GAMMs
184 penalized smoother functions are fitted for each treatment dependent on depth and with the
185 factors "Treatment", "Tray" and "Period" as covariates (equation 1), and with the residual variance
186 following a power function (dependent on depth) which is determined by the scale factor (δ) and
187 estimated in the same procedure.

188

189 $\text{Ln}(\% \text{Silt} + 1) = \alpha + f(\text{Depth} : \text{Treatment}) + \beta_1 \times \text{Treatment} + \beta_2 \times \text{Period} + \beta_3 \times \text{Tray} + \varepsilon$ (**Equation 1**)

190 with $\varepsilon \sim N(0, \sigma^2 \times |\text{Depth}_i|^{2 \times \delta})$

191

192 The resulting smoother functions for each treatment were statistically compared and the effect of
193 the factors "Treatment", "Period" and "Tray" were evaluated. The selection of the optimal model
194 was done by using (minimizing) the AIC statistic. The final model fit was checked on basis of plots of
195 residuals against fitted values as well as by checking for homogeneity of variance between the tested
196 factors.

197

198 **2.2.3. Autumn experiment**

199 Due to weather conditions we could deploy the lander for only one ~3-weeks period, *i.e.* week 40-44
200 in autumn (Table 1). The experimental setup was the same as in spring. Due to time constraints only
201 tubes which contained a living *Ensis* or an empty shell were sliced and compared. The slicing
202 procedure was slightly different from that what was used in the spring periods. When slicing the
203 cores of the spring experiment we observed that the sediment in the cores closely around a living *E.*
204 *directus* was darker in comparison to the areas further away from the shell. This suggested that the
205 mud enrichment primarily exists closely around the animal. We therefore changed the slicing
206 procedure, aiming to enhance the sensitivity of the comparison. Prior to slicing, we pushed a core of
207 35 mm diameter into the original 7 cm diameter tube so that it enclosed either the living *Ensis* or the
208 empty shell (Fig. 1). This resulted in an inner core which enclosed the living or dead *Ensis* with a
209 circle of sediment closely around it. The remainder of the core now contained only sediments at a
210 greater distance from the living *Ensis* or dead shell. This "core within a core" combination was sliced
211 separately, each in 1 cm layers up to the bottom of the core. Likewise as the spring cores, the

212 deepest core layers were pooled. Thus each tube provided two sets of samples; one from closely
213 around the living or empty *Ensis* shell i.e. "inner periphery" (0-35 mm) and the other from the "outer
214 periphery" (35-70 mm).

215 All sediment samples were treated in the same way as described in section 2.1. For each core
216 and each treatment (living or empty *Ensis*), the silt content of the inner and outer periphery were
217 layer by layer pairwise compared firstly using a Kruskal-Wallis test and secondly by fitting a
218 generalized additive mixed model (GAMM; Wood, 2006) describing the silt concentration being a
219 function of depth and with the factors "Core diameter" (Periphery), "Treatment" and "Tray" as
220 covariates (equation 2)

221

222 $\ln(\%Silt+1)=\alpha + f(\text{Depth} : \text{Periphery}) + \beta_1 \times \text{Periphery} + \beta_2 \times \text{Treatment} + \beta_3 \times \text{Tray} + \varepsilon$ (equation 2)

223 with $\varepsilon \sim N(0, \sigma^2 \times |\text{Depth}_i|^{2 \times \delta})$

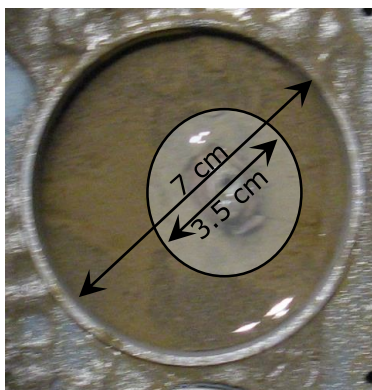
224

225 The depth layers were allowed to have different variances so that the residual variance followed a
226 power function with depth. The selection of the optimal model was done by using the AIC statistic.
227 Model fit was checked on basis of plots of residuals against fitted values as well as by checking for
228 homogeneity of variance between the tested factors.

229

230

231



232

233

234 Figure 1. Illustration of the slicing procedure applied. In the autumn experiment an inner core diameter 3.5 cm was pushed
235 into the tube just around the living or empty *Ensis* shell. This inner core formed the "inner periphery". The space outside
236 this inner core is called the "outer periphery". Both cores were sliced into 1 cm thick slices.

237

238 3. RESULTS

239 3.1 Coastal survey *Ensis directus*

240 **3.1.1 Sedimentary distribution**

241 The average median grainsize for all stations and transects in the boxcore survey was 222 μm (± 65
242 sd) with 5.13 % (± 4.3) silt ($< 63\mu\text{m}$). The two sampled sediment layers (0-5 cm and 5-10 cm) did not
243 differ in median grain size (t-test: $n=103$, $p=0.59$) nor in the percentage of silt (t-test: $n=103$, $p=0.41$).
244 The median grain size tended to increase in northward direction but only the most northern transect
245 differed significantly from the other transects (Tukey HSD, $p<0.05$). The percentages silt showed the
246 opposite trend although none of the transects differed significantly from each other in terms of
247 average silt percentage. The data also showed a trend in sediment characteristics perpendicular to
248 the coast. The median grainsize at the most offshore stations was higher (F-test; $p=0.014$) with lower
249 percentages of mud when compared to stations closer to the coast (F-test; $p=0.013$).

250

251 **3.1.2 Density distribution *E. directus***

252 Within the study area, there was an inverse relationship between the per transect averaged
253 densities of *E. directus* and geographical latitude (Figure 2). The most northern transect had lowest
254 densities and the most southern transects had the highest average density (Tukey HSD, $p<0.05$).
255 There was also a clear trend of the densities in the onshore-offshore direction. The lowest average
256 densities (22 m^{-2}) were invariably found at the most offshore stations (9-12). Highest average
257 densities ($177 \text{ individuals m}^{-2}$) were found at the intermediate stations (3-5) of most transects. The
258 mean density over all stations in the survey area was $90 \text{ individuals m}^{-2}$.

259

260 **3.1.3 Shell lengths *E. directus***

261 Mean shell length over the entire area was 99 mm (sd ± 19). There was no statistically significant size
262 difference between the transects in a north-south direction (Fig 2). In the across shore direction, the
263 size of the animals increased when moving from the coast. At the most offshore stations, shell
264 length was twice the size of the specimens at the inshore locations (F-test, $p<0.001$). Westwards
265 from station 6 the average shell lengths increased from $87 \pm 8.1 \text{ mm}$ to almost $160 \pm 15 \text{ mm}$.
266 Maximum size at the outer stations (7-12) was 154 mm and at the inner stations (1-6) 127mm.

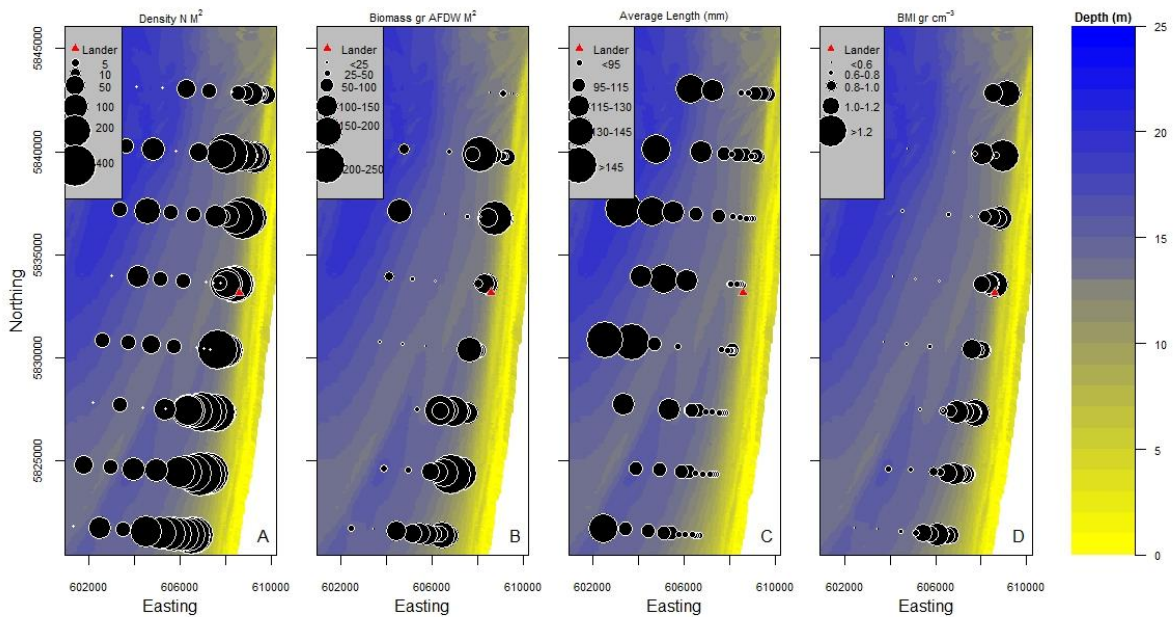
267

268 **3.1.4 AFDW and Body Mass Index (BMI) *E. directus***

269 Figure 2B shows the average biomass (AFDW m^{-2}) of *Ensis directus* over the investigated area and
270 illustrates the existence of spatial trends in both the along shore and across shore direction. Lowest
271 average biomass per square meter (23 gr m^{-2}) was found at the most northern transect (1) and the
272 highest average biomass ($121\text{-}144 \text{ gr m}^{-2}$) at the three southern transects (6-8). Biomass at the
273 intermediate transects ranged between 63 and 111 gr m^{-2} . In the across shore direction the average

274 biomass at the three outermost stations (9-12) was on average $52 \pm 24 \text{ gr m}^{-2}$, while the remaining
 275 inshore stations had an average biomass of $108 \pm 32 \text{ gr m}^{-2}$

276 The average BMI values for specimens from the various transects did not differ and ranged
 277 between 0.98 and 1.35. This is in contrast to the trends in BMI values in onshore-offshore direction.
 278 With an average value of 0.78 the bivalves at the furthest offshore stations appeared to have the
 279 lowest condition. The average BMI for more nearshore stations varied between 1.0 and 1.33 (Fig 2).



280
 281

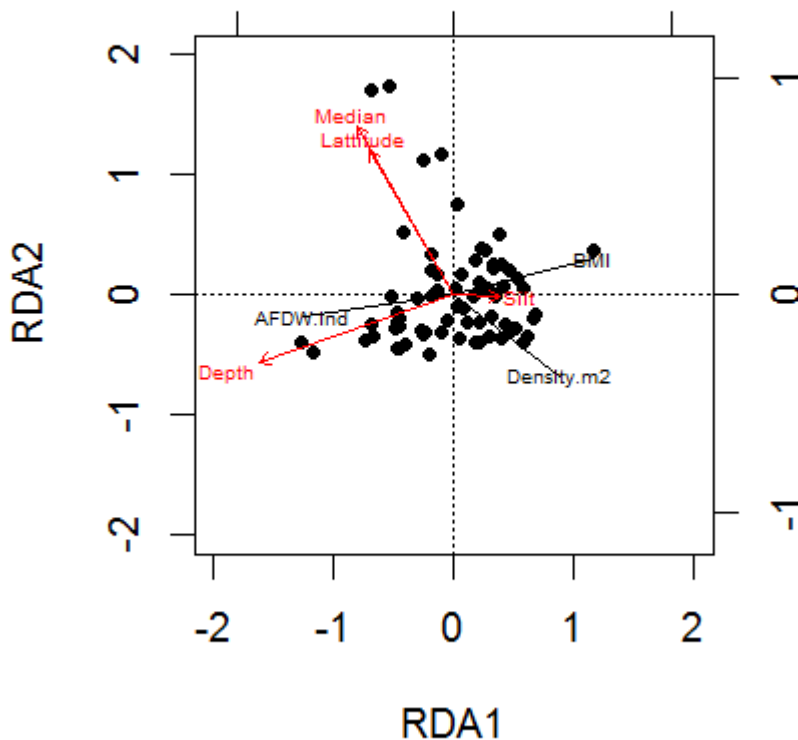
282

283 Figure 2. The main *E. directus* population characteristics as observed during the inventory in June 2011. Eight transects with each 12
 284 stations perpendicular to the coast were sampled with a boxcore. A) density in number m^{-2} ; B) biomass in gram AFDW m^{-2} ; C) average shell
 285 length in mm; D) Body Mass Index BMI. Lander position where the in situ experiments were done is drawn as a triangle.

286

287 3.1.5 *E. directus* population characteristics and environmental conditions

288 To find correlations between the characteristics of the *Ensis directus* population (size, density and
 289 condition) and the measured environmental factors (water depth, sediment data, latitude) a
 290 redundancy analyses (RDA) was performed. Because shell length and biomass are strongly
 291 correlated, biomass expressed as AFDW was used as descriptor of size. Figure 3 summarizes the
 292 results in a RDA triplot. The first two RDA axis explain 30% of the variation in the characteristics of
 293 the population along and across the surveyed coastal zone. Mean individual AFDW (biomass),
 294 density and BMI appear highly correlated to the water depth and sediment characteristics, together
 295 explaining 24% of the variance. Variance partitioning showed that depth explained 20% of the
 296 variance. Most of the remaining variance was explained by the sediment characteristics and latitude.
 297 Latitude by itself had a minor contribution and explained only 1.27% of the variance.



298

299 Figure 3. Graphical representation of a redundancy analyses of the main population characteristics (density, biomass and condition) with
 300 environmental parameters (median grainsize, depth and latitude). Highly correlated covariates (Mean Length) was omitted from this
 301 analyses on basis of the variance inflation factor.

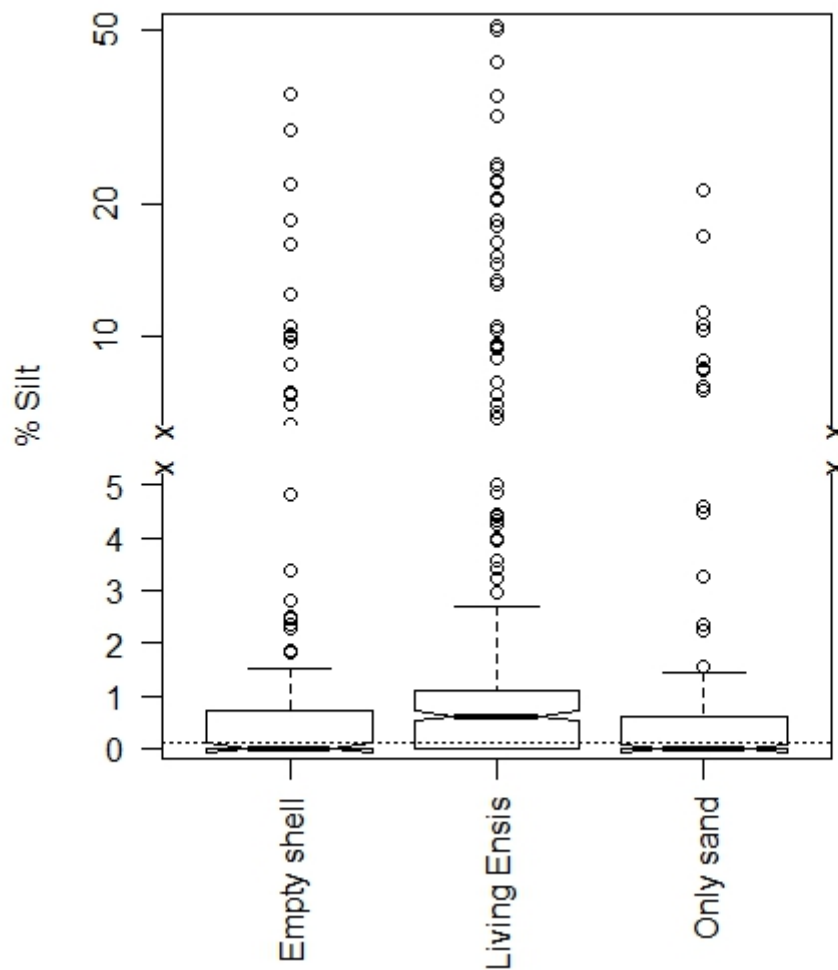
302

303 3.2. *In situ* silt burial experiments

304 3.2.1 Spring experiments

305 The grain size analyses showed that during the deployment the surface layers of all treatments
 306 became enriched in silt in comparison to the start condition of the experimental tubes (0.12%). The
 307 average silt content in the surface layer (0-5 cm) of all treatments had increased to 5.4 % but in
 308 many cores the silt percentages in the top layers was much higher. The average silt contents of the
 309 deeper layers (>5cm) of all tubes and treatments had increased from 0.12 to 0.21% which means
 310 that it had almost doubled. The average silt content in the cores containing a living *Ensis directus*
 311 ($2.8\% \pm 7.2$) was significantly higher than in the other two treatments (Figure 4; Kruskal_Wallace,
 312 $p \leq 0.05$). The average silt concentration in tubes with an empty shell ($1.9 \pm 5\%$) tended also to be
 313 higher than in tubes with only sand ($1.11\% \pm 3.14$) but this latter difference was not significant
 314 (Kruskal Wallace, $p = 0.38$). The box and whisker plots (Fig. 4) which tests for differences in median
 315 values confirm the above differences in average silt content. A pair wise comparison of the silt

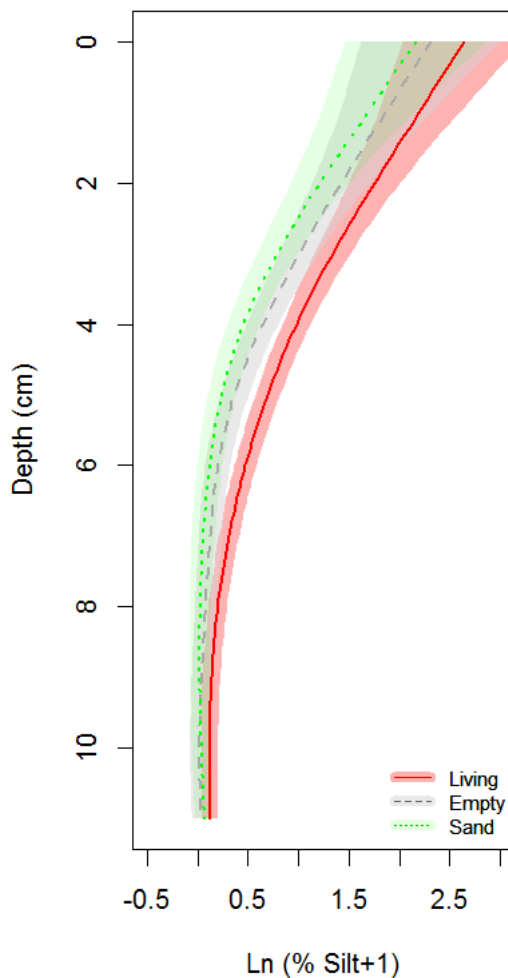
316 contents by treatment and separate layer showed that significant differences between treatments
317 were mainly found for sample slices taken deeper than 5 cm.



318
319 Figure 4. Comparison of the silt concentrations in the three treatments and depicted as notched box and whisker plot. The data for both
320 periods (week 10-14 and week 14-17 have been pooled). Thick black lines represent median values. Dotted line represents the average
321 percentage silt at the start of the experiment. Non overlapping notches of the boxes means that the difference between the medians is
322 significant.

323
324 To test which factors contributed to the observed differences, generalized additive mixed
325 models (GAMM; Wood, 2006) were fitted and compared to find the optimal combination of
326 explanatory variables. To remove any trend between residuals and fitted values it was necessary to
327 transform the silt data logarithmically and model variance as a power function of core depth. The
328 latter approach led to a 23% decrease in AIC statistic (Akaike's Information Criterion) when
329 compared to a model with equal variances for each layer. The results show that the smoother
330 function which described the silt content over sediment depth for the experimental tubes containing
331 a living *Ensis* was significantly ($p < 0.01$) different from the smoother functions which were estimated
332 for the other two treatments (Only sand, Empty Shell) (Figure 5). The factor "Period" did not have a

333 significant effect on the depth distribution of silt during the spring period. Thus in spring, both
 334 periods (weeks 10-14, 14-17) showed the same effect for the factor "Treatment", *i.e.* the function
 335 describing the silt distribution over sediment depth differed significantly in the presence of a living
 336 *Ensis* or an empty shell when compared to the control tubes (only sand), but the fitted smoother
 337 functions did not differ significantly between periods. The analyses furthermore demonstrated that
 338 the factor "Tray" had a significant effect on the silt content of the tubes. Especially the silt levels in
 339 Tray 2 were higher (+0.10%) when compared to Tray 1 and Tray 3 (+0.03%). Although this effect of
 340 "Tray" contributed significantly to the total explained deviance, it did not change the direction of the
 341 effect of the factor "Treatment" on the depth distribution of silt.
 342
 343



344
 345 Figure 5. A simplified graphical representation of the silt distribution over depth by treatment, *i.e.* disregarding the effect of the factor
 346 "Tray" for clarity of the plot. The treatments were "living *Ensis*", "empty shell" and "only sand". The tubes containing a living specimen had
 347 a significantly different smoother function describing the silt levels over depth in comparison to the other treatments. Shaded contour
 348 areas around the lines represents their 95% confidence interval around their fitted smoother function. Gamms were fitted with the
 349 package MGCV in R (Wood, 2006).

350

351 The results of the spring experiments show that in the presence of a living *Ensis* the modelled
 352 average percentage silt in a core had increased with 1.21% compared to cores with only sand, i.e.
 353 from 2.17% to 3.38% (Table 2), which is a relative increase of 56%. The silt contents in cores with a
 354 living *E. directus* compared to cores containing an empty shell increased with 0.86%, i.e. from 2.52%
 355 to 3.38% (Table 2), which is a relative increase of 34%. This shows that both a living *Ensis* and an
 356 empty shell led to higher sediment silt concentrations although the effect of a living specimen was
 357 more pronounced. These results suggest that the combined effect of the shell as physical object and
 358 the activity of the living *Ensis* contribute to enhanced sediment silt contents.

359
 360

361 **3.2.2. Autumn experiments.**

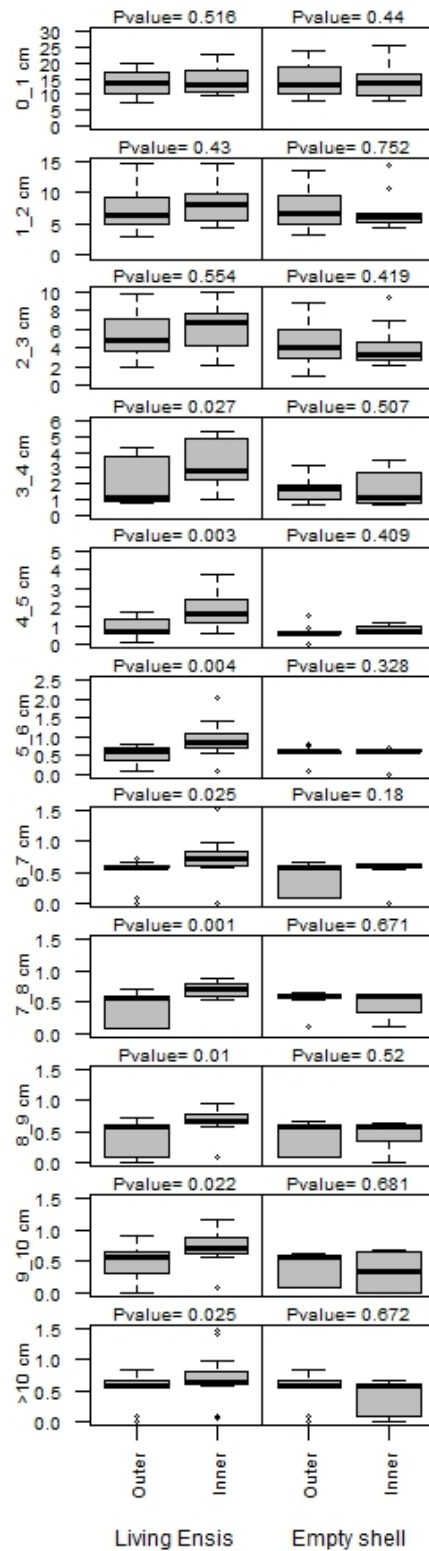
362 In autumn we changed the slicing procedure, i.e. we sliced a small 3.5 cm core taken from within the
 363 original 7 cm core separately, as explained in section 2.2.3. The layer by layer comparison, showed
 364 that there was no difference in the silt contents over depth between the inner and outer periphery
 365 in tubes containing an empty shell (Fig. 6; post hoc Tukey HSD test). In tubes containing a living *Ensis*
 366 the inner periphery (3.5 cm) had significantly higher silt concentrations when compared to the outer
 367 periphery. This difference was present in all layers deeper than 3 cm. For layers shallower than 3 cm,
 368 no significant difference was observed.

369

Treatment	Spring	Autumn	
		Inner periphery	Outer periphery
	% silt	% silt	% silt
Only sand	2.17	NA	NA
Empty Shell	2.52	3.15	2.94
Living <i>Ensis</i>	3.38	3.50	3.30

370

371 Table 2 From the GAMM model back calculated average transformed silt contents over all layers and replicates within one type of
 372 treatment. Results for both the spring period and the autumn period are given.



373

374 Figure 6. Pairwise comparison of silt contents (%silt) in the separate sediment layers in the inner and outer periphery of tubes with a living
 375 *Ensis directus* (left panel) and of tubes containing an "empty shell" (right panel) in the autumn period. For each treatment and depth layer
 376 the silt levels are compared on basis of boxplots. For each comparison the estimated P value on basis of a post hoc Tukey HSD test
 377 between inner and outer periphery is given in the top left corner.

378

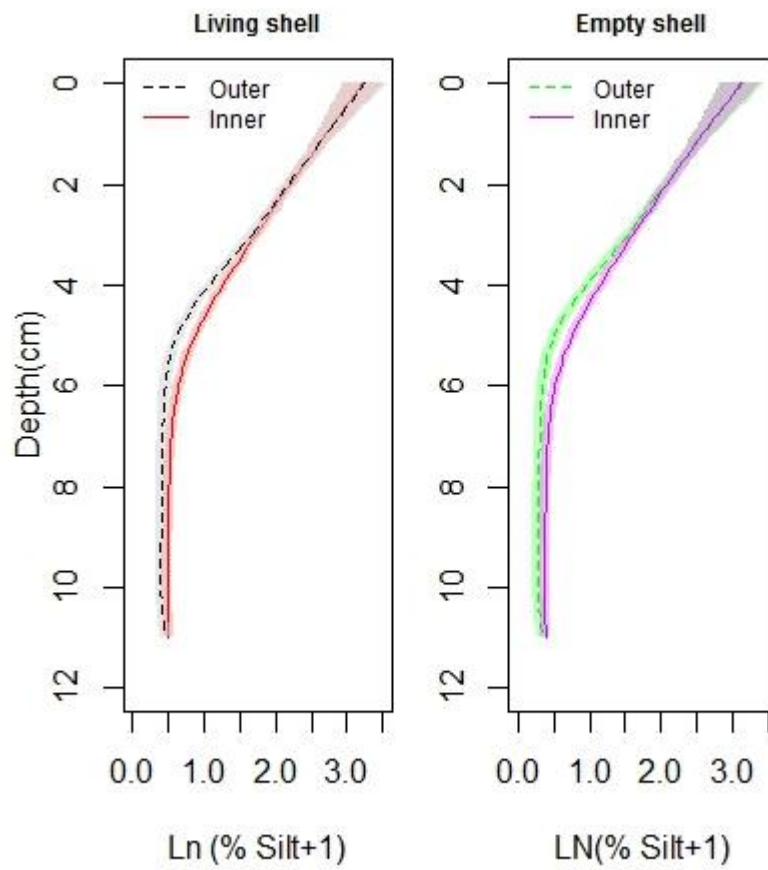
379 Like for the "spring" experiment, a GAMM model was fitted which described the depth
380 distribution of silt for each of the treatments. Model selection was based on the AIC. Model fit was
381 checked by plotting residuals against fitted values. It appeared that the depth dependent variance of
382 the silt content fitted best to a power function. This addition lowered the AIC with 10% when
383 compared to a model with uniform variance over depth. This together with a logarithmic
384 transformation ($\ln \%Silt + 1$), removed the strong trend between residuals and fitted values, implying
385 that the model is accurate in describing the depth distribution of silt over the full depth range.

386 The smoother functions estimated for the inner and outer periphery differed significantly
387 ($p < 0.01$) with the outer periphery having lower silt contents for both the tubes with a living *Ensis* and
388 an empty shell. The recalculated silt profiles derived from these estimated GAMM smoother
389 functions, suggest that the difference between the inner and outer periphery of living and an empty
390 shell is about equal (0.20-0.21, respectively). This indicates that the presence of a physical object (or
391 living *Ensis* or empty shell) both promote burial of silt closely around the object.

392 The increase in silt content in the tubes with a living *Ensis* is larger than in tubes with an empty
393 shell. The difference between average silt percentages in the "living *Ensis*" (3.40 %, inner + outer;
394 Table 2) and the "Empty shell" (3.05 %, inner + outer; Table 2) tubes was 0.35% which equals an
395 relative increase of 11% in sediment silt content generated by a living specimen. This is a small value
396 when compared to the equivalent effect of a living *Ensis* found in the spring period (i.e. 34%), but it
397 supports the spring observation that around a living *Ensis* the silt contents are indeed higher than
398 around an empty shell and that the effect is especially notable closely around the shell object as was
399 initially observed in spring.

400 Because of the change of the set-up of the autumn experiment, i.e. the differentiation
401 between inner and outer core and the absence of "only sand" controls, we were unable to test the
402 difference between spring and autumn results statistically.

403



404

405 Figure 7. Comparison of the fitted GAMMs describing the depth distribution of silt in both treatments in autumn. Inner periphery (solid
 406 line); outer periphery (dotted line). Shaded areas represent 95% confidence limits around the fitted smoother function. Gamms were
 407 fitted with the package MGCV in R (Wood, 2006).

408

409

410

411

412 4. DISCUSSION

413 During our synoptic survey we found lowest densities of *E. directus* at the stations furthest
414 offshore. The average shell length was almost double the size of those found close to the shore. The
415 offshore animals are mainly larger and older (ring counts, Cardoso *et al.*, 2013) suggesting that
416 survival is better here than in the shallow nearshore area. The low BMI (0.78) of the offshore
417 animals, however, suggests that conditions for (tissue) growth are sub optimal compared to the
418 shallow nearshore where the highest densities (177 individuals m⁻²) and highest BMI values (1.0 and
419 1.33) were found. This pattern is remarkable as this shallow inshore zone is characterized by high
420 concentrations of suspended silt and overlaps with the turbidity maximum zone (TMZ; van der Hout
421 *et al.*, 2015) as observed by satellite (e.g. RIKZ 2002). It is repeatedly assumed that high suspended
422 silt levels have a negative effect on growth and production of filter-feeders like bivalves (Cranford *et*
423 *al.*, 1992; Grant & Thorpe, 1991; Grémare *et al.*, 1998; Witbaard *et al.*, 2001). Other studies,
424 however, demonstrate positive effects of silt on growth, like Kamermans *et al.* (2013) who observed
425 a slight positive effect of suspended silt on growth in *Ensis directus*. Our field data on abundance and
426 BMI confirm such positive effects. Both the high nearshore densities and high body mass conditions
427 (BMI) coincide with locations where high silt contents were found in water and sediment (Fig. 2).
428 Local hydrographical phenomena seem to be the unifying process which can explain the
429 simultaneous existence of the Turbidity Maximum zone (TMZ), the high *E. directus* densities, their
430 good condition and the high sediment silt contents.

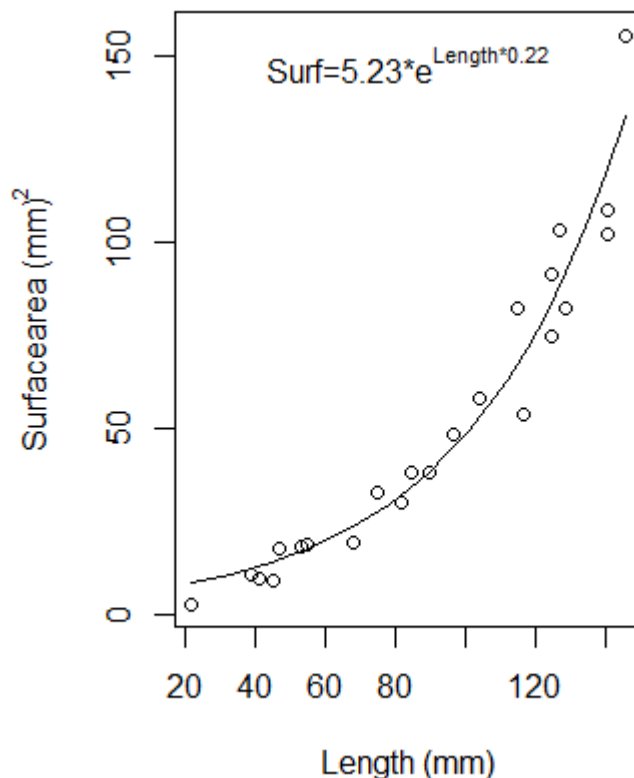
431 On basis of physical characteristics of mud deposition and erosion in the Dutch coastal zone,
432 Kleinhans *et al.* (2005) concluded that bioturbation may explain the presence of mud in deeper
433 sediment layers. The authors did not deliberate which (group of) organism(s) was responsible for the
434 deep mixing. Taking into account the observations by Armonies & Reise (1999) near the island of Sylt
435 and data from our spatial survey, *E. directus* was considered a probable candidate. Our in-situ
436 experiments showed that in both spring periods the average percentage silt in cores holding a living
437 *E. directus* or a vertically positioned empty shell had increased significantly, when compared to cores
438 with only sand. These results suggest that the combined effect of both the shell as obstacle and the
439 activity of the living *Ensis* contribute to enhanced silt contents. The autumn experiments confirmed
440 this conclusion: especially the sediments closely around a living *Ensis* contained significantly higher
441 percentage of silt (Table 2; Fig. 6; Fig. 7) than the outer part. A possible reason for the observed
442 seasonal difference in silt entrapment could have been the relatively calm weather in spring
443 compared to the autumn period, but could also be related to seasonal differences in activity of the
444 living *Ensis* as well as to qualitative differences of the suspended material filtered by *Ensis*. The aim
445 of the experiments was to test the hypothesis that *Ensis directus* promotes the burial of silt. The

446 structural constraints of the lander made that the top of the trays were positioned 54 cm above the
447 seafloor. It is likely that this has had consequences for the amounts of suspended material passing
448 over the trays as the concentration of silt is a function of height above the seafloor. The
449 concentration gradient follows a Rouse profile (van der Hout *et al*, submitted, this volume) with
450 decreasing concentrations higher above the bottom. This implies that the silt concentrations above
451 the experimental trays in the lander were an underestimation of the actual concentrations at the
452 seafloor-water interface and that the calculated silt burial rates are a conservative estimate. As a
453 consequence of their elevated position, the height of the trays above the seafloor can easily be
454 affected by the tilt of the lander. Tilt measurements (1-2.5 degrees) in the spring period suggest that
455 the height of a tray above the seafloor could have been reduced with 4.5 cm. In autumn a peak tilt
456 value of 9 degrees, measured during a storm period (Oct 19-24th 2010), could have led to a reduction
457 in height of 15 cm. This maximum change in height could only be reached if the orientation of the tilt
458 matched the length orientation of the tray. For trays oriented not parallel, the change in height
459 above the seabed will be smaller. In spite of this short period with increased tilt between Oct 19th
460 and October 24th 2010, we could not prove that this resulted in higher silt concentrations in the core
461 slices taken from the autumn experiment. It is more likely that the rougher conditions directly or
462 indirectly (e.g. via activity of *Ensis* itself) influenced silt burial.

463 The results from the spring and autumn deployments show that both living and dead *Ensis directus*
464 contribute to the burial of silt. Based on these results and the ecology of this species we envision 3
465 ways in which *E. directus* contributes to siltation of the sediment, e.g. by i) increasing bottom
466 roughness, ii) biodeposition, and iii) biomixing. In the next paragraph we discuss evidence for each of
467 these mechanisms.

468 The first mechanism refers to the increased bottom roughness generated by the partially
469 protruding shells and siphons of *Ensis directus* which affect the flow conditions and sedimentation of
470 particles. Experimental studies showed variable results, Gutierrez & Iribarne (1999) reported that
471 protruding shells stabilized sediment while others (Willows *et al.*, 1998; Widdows *et al.*, 1998)
472 mentioned the opposite. Later Friedrichs *et al.* (2000) showed that the sedimentation-erosion
473 balance is determined by the Roughness Density factor (RD) *i.e.* the percentage of bottom surface
474 covered by "obstacles". They demonstrated that in coarse sand at relatively low current speeds, a RD
475 value >0.08 led to a skimming flow over obstacles even when they extend 3.5 cm into the Benthic
476 Boundary Layer (BBL). In such conditions the flow within the obstacle bed is strongly reduced
477 provoking sedimentation (Graf & Rosenberg, 1997) as the BBL *i.e.* the zone with the erosion-inducing
478 high Reynolds stresses, is uplifted. RD values calculated on basis of the relationship between shell
479 length and the surface area of the cross section of the shell top segments (Fig. 8) and the *E. directus*

480 densities in 2011, ranged between 0.0035 and 0.008. The lowest RD values were found at the three
 481 outermost stations with low densities of large animals. Highest average RD values occurred between
 482 station 3 and 8 at a distance between 1 -3 km from the coast (LWM). These values are clearly below
 483 the threshold where skimming flow conditions normally evolve (Friedrichs *et al.*, 2000). However,
 484 most of the animals sampled in 2011 belonged to the 2009-cohort. They were 2 years old and since
 485 they had settled already experienced significant mortality (Witbaard *et al.*, 2015). In September
 486 2009 initial densities of 2300 individuals m⁻² were found. By February-March 2010 densities had
 487 decreased to 500 individuals m⁻². Based on these two density estimates and their associated
 488 average shell sizes (Witbaard *et al.*, 2015) the RD values would have ranged between 0.44 and 0.09,
 489 respectively. These values surpass the critical values as identified by Friedrichs *et al.* (2000) and
 490 illustrate that in the early phase of population development (with high densities of *Ensis directus*)
 491 skimming flow conditions can easily evolve and thus promote the accumulation of fine sediments on
 492 the seabed. Our data on the population development and growth of *Ensis directus* in the area
 493 (Witbaard *et al.*, 2015) suggests that their effect on near bottom flow is largest in the second year of
 494 a cohort because that combines high densities with sufficiently large shell cross section surface
 495 areas.



496

497 Figure 8. The morphometric relationship between shell length and cross sectional surface area at the shell top of *Ensis directus* which is at
 498 or extends from the sediment surface. This relationship was used to estimate the roughness density factor of the coastal *E. directus*
 499 population as found in the inventory and in different phases of development as described in Witbaard *et al.*, 2015.

500

501 A second process which may contribute to elevated silt levels in the sediment is the
502 biodeposition of suspended material by *E. directus*. While feeding fine suspended particles are
503 retained on their gills and particles not suited as food are coagulated and excreted as faeces or
504 pseudofaeces (biodeposits). Sinking velocity and erosion threshold of these bio-deposits depend on
505 diet and pellet size (Giles & Pilditch, 2004). Coagulation of particles may double their sinking
506 velocities (Zhou *et al.*, 2014) and with that their deposition-erosion characteristics (see also Oost,
507 1995). Since the amount of inorganic matter appears an important determinant for sedimentation,
508 not only seasonal, but also short term effects (tidal, storm) on pellet composition and sedimentation
509 rate can be expected. Oost (1995) reported that biodeposits were resistant to disintegration and
510 remained intact over several tidal cycles. Thus depending on flow conditions, faecal pellets may
511 accumulate at the seabed as we observed at the surface of boxcore samples in 2011 (Fig. 9).

512



513

514

515 Figure 9. Photograph taken from the sediment surface of a boxcore with faecal pellet accumulations. The weather conditions were calm in
516 the 2011 (June) survey. The boxcore contained living *E. directus* .

517

518 Faeces and pseudo-faeces production of *Ensis directus* depends on its clearance and
519 assimilation rate, but also on the food and silt content (Kamermans *et al.*, 2013) of the water. The
520 authors reported that at 18°C and a silt (kaolin) concentration of 0 to 150 mg L⁻¹, the clearance rate
521 of *E. directus* ranged from 0.20-0.36 L hr⁻¹ in small (33-75 mm) individuals and from 3.7 to 5.1 L hr⁻¹ in
522 larger (>100 mm) specimens. A sharp reduction (~70%) in clearance rate occurred if the silt (kaolin)
523 concentration surpassed 300 mg L⁻¹ (Kamermans *et al.*, 2013). On basis of these size dependent
524 clearance rate estimates, and the size frequency distribution of *E. directus* densities (90 m⁻²) in 2011
525 in the study area (Witbaard *et al.*, 2015), we estimate that the average volume of water filtered by

526 the local *E. directus* population was $126 \text{ L hr}^{-1}\text{m}^{-2}$. This means that at a water depth of 10 m, 30% of
527 the water column was filtered once a day and its SPM potentially made available for deposition in de
528 form of pseudofaeces or faecal pellets. The amount of silt potentially processed along this way can
529 be estimated from the filtered volume and the average SPM concentration in the coastal zone. Van
530 der Hout *et al.* (2015) detected a persistent Turbidity Maximum Zone (TMZ) with on average 150 mg
531 L^{-1} SPM (Witbaard *et al.*, 2015) at a distance of 0.5 - 3 km from the coast. The near-bottom SPM
532 concentrations at more offshore locations were considerably lower ($\sim 20\text{-}50 \text{ mg L}^{-1}$; van der Hout *et*
533 *al.*, 2015). For this calculation we therefore conservatively assumed that the average bottom water
534 SPM concentration was 50 mg L^{-1} in the first 6 km from the shore. If this amount of SPM was
535 completely extracted from the estimated filtered volume ($126 \text{ L hr}^{-1} \text{ m}^{-2}$) and excreted as faeces or
536 pseudofaeces, a maximum of $6.3 \text{ gram SPM hr}^{-1} \text{ m}^{-2}$ was potentially aggregated into bio-deposits.
537 This equals an average of $70 \text{ mg SPM individual}^{-1} \text{ hour}^{-1}$, which is comparable to biodeposition rates
538 measured under mussel farms (Barnes, 2006), but 10-20 times higher than estimates for natural
539 populations of filter-feeding bivalves such as *Mytilus edulis* ($17\text{-}86 \text{ mg day}^{-1}$; Callier *et al.*, 2006),
540 *Modiolus modiolus* (40 mg day^{-1} ; Navarro & Thompson, 1997) or *L. elliptica* ($161 \text{ mg ind}^{-1} \text{ day}^{-1}$; Ahn,
541 1993).

542 Extrapolation of above biodeposition rates for *Ensis directus*, to the entire Dutch coast with 12
543 billion individuals (Goudswaard *et al.*, 2013) would suggest that on a daily basis potentially 0.12
544 Mton SPM can be deposited by this species. In comparison to the estimated SPM transport along the
545 Dutch coast ($22\pm 10 \text{ Mton yr}^{-1}$; de Kok, 2004) this is a remarkable high value. There are several
546 reasons to assume that this estimate is too high. We estimated the daily biodeposit production on
547 basis of clearance rates which were measured at 18°C (Kamermans *et al.*, 2013) while the average
548 water temperature was 12°C in the study area. Activity of bivalves in a temperate environment is
549 inversely related to temperature leading to *e.g.* a 50% decrease in average valve gape (80->40%) if
550 temperatures drop below 10°C (Witbaard *et al.*, 2013). As water temperatures are below 10 degrees
551 during 4 months (Witbaard *et al.*, 2015), an overestimation of filtration rates and biodeposit
552 production is likely. A further overestimation possibly occurred by ignoring that SPM concentrations
553 surpassing 300 mg L^{-1} suppress clearance rates (Kamermans *et al.*, 2013). Measurements at the
554 experimental field site showed that this occurs for 11% of the measured time (Witbaard *et al.*, 2013).
555 Valve gape data for *Ensis directus* measured over a 254 day period (Witbaard *et al.*, 2013)
556 furthermore showed that for 54% of the time, the average valve gape was below 75% showing that
557 *E. directus* is not continuously filtering with fully open siphons at maximum rates. These
558 observations are supported by those of Miller *et al.* (1992) who found that siphon extension which is
559 a clear indication of filtration rate, changed regularly in a variable flow.

560 Another factor which might lead to a reduction in biodeposit production is a limitation in the
561 availability of SPM near the seabed. Limited availability of SPM might be a consequence of high
562 bivalve densities itself, depleting the source, as well as that the dense beds cause skimming flow to
563 develop. Skimming flow might lead to food limitation (Friedrichs et al, 2000) and with that to
564 behavioural responses and reduced filtration and thus biodeposit production rates. Palmer (1994)
565 suggests that the reduced growth in *E. directus* (>2000 M⁻²) he observed were related to density
566 dependent processes which implied that the supply of food was limiting. That food limitation in
567 shell fish beds occur is, among others, illustrated by Jonsson et al (2005). They measured a 5-30%
568 downstream decrease in near bottom chlorophyll over a *Cerastoderma* shellfish bed, because
569 exhalent (already filtered) water mixed with the horizontal primary particle rich water flow. We have
570 no reason to assume that this process act differently above a dense *Ensis* bed.

571

572 Based on the above mentioned reasons, *i.e.* the strong temperature effect on valve gape, the
573 time spend (54%) by *Ensis* with partially closed valves (<75% valve gape), the 70% reduction in
574 filtration rates at high SPM concentrations and the potential food-particle limitation in dense beds,
575 the estimated potential biodeposit production might be 50% too high. But even despite such
576 correction it still implies that the *E. directus* population along the Dutch coast acts as an effective
577 biofilter having a considerable influence on the mass balance and sedimentation-resuspension
578 behaviour of fine suspended particles in the coastal area.

579 The above two processes (increased bottom roughness and biodeposition) both enhance
580 deposition of silt at the sediment surface, while biodeposition in the form of pellets also lowers the
581 resuspension rate. Equally relevant for the observed siltation of the coastal zone are processes that
582 lead to burial of silt, like the burrowing behaviour of *Ensis*. Upon disturbance, *E. directus* retracts
583 and buries itself rapidly and completely below the sediment surface (Trueman, 1967; Drew, 1907).
584 During retraction, water is expelled from the mantle cavity through the fourth aperture (Holme,
585 1951), a small opening midway the fused mantle edges that acts as a "safety valve" (Trueman, 1967).
586 If this water contains fine particles (food or silt from the gills and mantle cavity) this will be injected
587 deeper in the sediment and locally elevate the silt content. Maybe even more important is the
588 sediment movement caused by the burrowing action itself. To reduce drag while burying, *Ensis*
589 fluidizes its surrounding sediment (Winter *et al.*, 2012). The descending animal pulls superficial
590 bottom material into the pit formed by the "collapsing" sediment above and around itself. These
591 biomixing processes both contribute to the burial of fine particles and faecal pellets originating from
592 the sediment surface. During the sampling campaigns in the coastal area we noticed a fourth
593 mechanism by which silt penetrates the sediment. In boxcore samples we spotted empty shells of *E.*

594 *directus* still in their natural vertical position but with their soft tissues replaced by fine sediment.
595 Empty shells had evidently acted as a sediment trap and the accumulated material had silt
596 concentrations up to 52 %, a 10 times higher concentration than the average sediment silt content in
597 that zone. This route may also lead to a rapid increase in bottom silt contents.

598

599 Although the separate mechanisms need further scrutiny and quantification, together they
600 match with our observations that the presence of living and dead *E. directus* can lead to
601 accumulation of silt at the seabed and into the deeper sediment layers. The importance of this burial
602 for the silt balance in the coastal zone can be appreciated when the increase in the volume % of silt
603 in the in situ PVC tubes is back calculated to a total mass of silt with an assumed specific weight of
604 2.798 gram cm⁻³. If the calculated total mass of buried silt as derived from the spring experiment is
605 extrapolated to an annual period and a population size along the entire Dutch coast of 72 billion
606 individuals (Goudswaard et al., 2013) about 6 Mton of fine particles became (temporally) buried. On
607 basis of the silt increase measured in the autumn experiment we estimate that 0.6 Mton was buried,
608 a factor 10 lower than in spring. This difference is likely to be linked to the difference in weather in
609 spring and autumn as well to differences in filtration activity related to qualitative differences in
610 suspended matter caused by the seasons (Figure 2D in Witbaard et al., 2015). The estimated annual
611 burial of SPM (0.6-6 Mton/yr) by *Ensis* fits within the range of biodeposit production by *Mytilus* in
612 the Dutch Wadden Sea (2.6 to 15.1 Mton; Oost 1995). Thus while daily biodeposit production
613 estimates, based on filtration rates of *Ensis* appears to be two times too high, the estimates based
614 on the measured silt burial compare well to the magnitude of biodeposit production by *Mytilus* in
615 the neighbouring Wadden Sea ecosystem.

616 Observations suggest that the coastal sediment acts as a (temporary) storage of fine particles.
617 The seasonal trends in median grain size and of volume % silt at the lander site (Witbaard *et al.*,
618 2013, Witbaard *et al.*, 2015) indicate that this storage is subject to large seasonal variation which
619 corroborates the above estimates of seasonal differences in burial of silt and which also has been
620 demonstrated for intertidal areas in the Wadden Sea (Oost, 1995).

621 The burial of silt (0.6 and 6 Mton yr⁻¹) by *E. directus* equals up to ± 30% of the annual SPM
622 transport (22±10 Mton yr⁻¹; de Kok, 2004; van der Hout *et al.*, 2015) along the Dutch coast and
623 between 45 and 85% of the annual influx (7-11 Mton; Nauw *et al.*, 2014) into the western Wadden
624 Sea via the Marsdiep tidal inlet. These percentages indicate that the coastal *E. directus* population
625 has a large impact on the ecological functioning of Dutch coastal and estuarine ecosystems.

626 Part of the suspended material along the Dutch coast originates from the continuous
627 foreshore and beach nourishments (48x10⁶ m³ between 2012-2015: RWS, 2014). The associated

628 increase in SPM is assumed to have negative effects on basic ecosystem functions such as primary
629 and secondary production (Duin *et al.*, 2007). Our results suggest that especially relative young and
630 dense populations of *E. directus* may contribute to the mitigation of such effects as we found
631 evidence that both alive individuals as well as empty shells (still in their vertical position) facilitate
632 silt burial. Settlement of *E. directus* may even be promoted by the availability of newly created
633 "virgin" unstructured sediments which are continuously generated by these nourishments along the
634 Dutch coast (Witbaard *et al.*, 2015). Supporting evidence for this idea comes from a large scaled field
635 experiment in the Wadden Sea where *E. directus* spat showed similar preference (van der Heide *et*
636 *al.*, 2014). Such preference of *Ensis* spat might imply that the ongoing beach nourishments actually
637 promote settlement and population growth of *E. directus* along the Dutch coast. In the context of
638 ongoing beach maintenance works it is critical to understand the potential relationship between *E.*
639 *directus* settlement and coast maintenance. A thoughtful nourishment strategy which leads to
640 successful settlement and high *E. directus* densities can potentially counteract the negative effects of
641 increased SPM levels as we have found that *Ensis directus* is able to increase sedimentation and
642 burial of silt. Such feedback mechanisms may underlay a sustainable nourishment practice which
643 contributes rather than is in conflict with the conservation/restoration of natural values of the
644 coastal habitat of submerged breakerbanks (H1110).

645

646 **Acknowledgments.**

647 This work has been made possible by financial support of a grant of Ecoshape (project nos. NTW3.1–
648 NTW2.5) within the framework of BWN and NIOZ itself. The practical work could not have been
649 done without the enormous input of the crews of RV “Pelagia” and RV “Navicula”. We thank Carola
650 van der Hout for her help on board. This work preceded a two years project funded by the la Mer
651 foundation.

652

653 **5. References**

- 654 Ahn, I.Y., 1993. Enhanced particle flux through the biodeposition by the Antarctic suspension-feeding
655 bivalve *Laternula elliptica* in Marian Cove, King George Island. *J. Exp. Mar. Biol. Ecol.* 171, 75-
656 90.
- 657 Arias, A., Anadon, N., 2012. First record of *Mercenaria mercenaria* (Bivalvia: Veneridae) and *Ensis*
658 *directus* (Bivalvia: Pharidae) on Bay of Biscay, Iberian Peninsula. *J. Shellfish Res.* 31 (1), 57-60.
- 659 Armonies, W., 2001. What an introduced species can tell us about the spatial extension of benthic
660 populations. *Mar. Ecol. Prog. Ser.* 209, 289-294.

661 Armonies, W., Reise, K., 1999. On the population development of the introduced razor clam *Ensis*
662 *americanus* near the island of Sylt (North Sea). *Helgoländer Meeresun.* 52, 291-300.

663 Barnes, P., 2006. Shellfish culture and particulate matter production and cycling: A literature review.
664 Report for BC Aquaculture Research and Development Committee. AE 02.03-02.01, 78pp.

665 Cadee, G.C., 2000. Herring gulls feeding on a recent invader in the Wadden Sea, *Ensis directus*. In:
666 Harper, E.M., Taylor, J.D & Crame (eds) *The evolutionary Biology of the bivalvia*. Geological
667 society London. Special publications 177, 459-464.

668 Callier, M.D., Weise, A.M., McKindsey, C.W., Desrosiers, G., 2006. Sedimentation rates in a
669 suspended mussel farm (Great-Entry Lagoon, Canada): Biodeposit production and dispersion.
670 *Mar. Ecol. Prog. Ser.* 322, 129-141.

671 Cardoso, J.F.M.F., Nieuwland, G., Witbaard, R., van der Veer, H.W., Machado, J.P., 2013. Growth
672 increment periodicity in the shell of the razor clam *Ensis directus* using stable isotopes as a
673 method to validate age. *Biogeosciences* 10, 4741-4750.

674 Cranford, P.J., Gordon, D.C., 1992. The influence of dilute clay suspensions on sea scallop
675 (*Placopecten magellanicus*) feeding activity and tissue growth. *Neth. J. Sea Res.* 30, 107-120.

676 Dannheim, J., Rumohr, H., 2012. The fate of and immigrant: *Ensis directus* in the eastern German
677 Bight. *Helgol. Mar. Res.* 66, 307-317.

678 Dauvin, J.C., Ruellet, T., Thiebaut, E., Gentil, F., Desroy, N., Janson, A.L., Duhamel, S., Jourde, J.,
679 Simon, S., 2007. The presence of *Melinna palmata* (Annelida: Polychaeta) and *Ensis directus*
680 (Mollusca: Bivalvia) related to sedimentary changes in the Bay of Seine (English Channel,
681 France). *Cah. Biol. Mar.* 48, 391-401.

682 De Kok, J.M., 2004. Slib transport langs de Nederlandse kust-Bronnen, fluxen en Concentraties.
683 Report RIKZ/OS/2004.148w.

684 Dekker, R., Beukema, J.J., 2012. Long-term dynamics and productivity of a successful invader: The
685 first three decades of the bivalve *Ensis directus* in the western Wadden Sea. *J. Sea Res.* 71, 31-
686 40.

687 Drew, G.A., 1907. The habits and movements of the razor-shell clam, *Ensis directus*, *Con. Biol. Bull.*
688 XII (3), 127-142.

689 Duin C.F. van, Gotjé, W., Jaspers, C.J., Kreft, M., 2007. MER Winning suppletiezand Noordzee 2008
690 t/m 2012. Grontmij Hoofdrapport, Definitief. 13/99080995/CD, revisie D1 242 pp, Grontmij,
691 Houten.

692 Friedrichs, M., Graf, G., Springer, B., 2000. Skimming flow induced over a simulated polychaete tube
693 lawn at low population densities. *Mar. Ecol. Prog. Ser.* 192, 219-228.

694 Giles, H., Pilditch, C.A., 2004. Effects of diet on sinking rates and erosion thresholds of mussel *Perna*
695 *canaliculus* biodeposits. Mar. Ecol. Prog. Ser., 282, 205-219.

696 Goudswaard, P.C., Perdon, K.J., Jol, J., van Asch, M., Troost, K., 2013. Het bestand aan commercieel
697 belangrijke schelpdiersoorten in de Nederlandse kustwateren in 2013. IMARES rapport
698 C133/13, 38pp.

699 Graf, G., Rosenberg, R., 1997. Bioresuspension and biodeposition: A review. J. Marine Syst., 11, 269-
700 278.

701 Grant, J., Thorpe, B., 1991. Effects of suspended sediment on growth, respiration and excretion of
702 the soft-shell clam (*Mya arenaria*). Can. J. Fish. Aquat. Sci., 48, 1285-1292.

703 Grémare, A., Amouroux, J.M., Chabeni, Y., Charles, F., 1999. Experimental study of the effect of
704 kaolinite on the ingestion and the absorption of monospecific suspensions of *Pavlova lutheri*
705 by the filter-feeding bivalve *Venus verrucosa*. Vie Milieu, 48(4), 295-307.

706 Gutiérrez, J., Iribarne, O., 1999. Role of Holocene beds of the stout razor clam *Tagelus plebeius* in
707 structuring present benthic communities. Mar. Ecol. Prog. Ser. 185, 213-228.

708 Holme, N.A., 1951. The identification of British species of the genus *Ensis* Schumacher
709 (Lamellibranchiata). J. Mar. Biol. Ass. U.K. 29 (3), 639-647.

710 Jonsson, P.R, J.K.Petersen, O.Karlsson, L.O. Loo, S. Nilsson, 2005. Partial depletion above
711 experimental bivalve beds: In situ measurements and numerical modelling of bivalve filtration
712 in the boundary layer. Limnol. Oceanogr. 50(6): 1989-1998.

713 Kamermans, P.E., Brummelhuis, E., Dedert, M., 2013. Effect of algae- and silt concentration on
714 clearance- and growth rate of the razor clam *Ensis directus*, Conrad. J. Exp. Mar. Biol. Ecol.,
715 446, 102-109.

716 Kleinhans, M.G., Montfort, O., Dankers, P.J.T., Van Rijn, L.C. and Bonne, W., 2005. Mud dynamics on
717 the shoreface and upper shelf, Noordwijk, The Netherlands. EU-Sandpit end-book, Ed. Leo van
718 Rijn, Aqua Publications, The Netherlands, paper Z, 1-15.

719 Miller, D.C., Bock, M.J., Turner, E.J., 1992. Deposit and suspension feeding in oscillatory flows and
720 sediment fluxes. J. Marine Syst. 50, 489-520.

721 Nauw, J.J., Merckelbach, L.M., Ridderinkhof, H., van Aken, H.M., 2014. Long-term ferry-based
722 observations of the suspended sediment fluxes through the Marsdiep inlet using acoustic
723 Doppler current profilers. J. Sea. Res. 87, 17-29.

724 Navarro, J.M., Thompson, R.J., 1997. Biodeposition by the horse mussel *Modiolus modiolus* (Dillwyn)
725 during the spring diatom bloom. J. Exp. Mar. Biol. Ecol., 209, 1-13.

726 Oksanen, J., Guillaume Blanchet, F., Kindt, R., Legendre, P., Minchin, P.R., O'Hara, R.B., Simpson, G.L.,
727 Solymos, P., Henry, M., Stevens, H., Wagner, H. 2013. Vegan: Community Ecology Package. R
728 package version 2.2-1. <http://CRAN.R-project.org/package=vegan>

729 Oost, A.P., 1995. The influence of biodeposits of the blue mussel *Mytilus edulis* on fine grained
730 sedimentation in the temperate climate Dutch Wadden Sea, pp 359-401. *In* Dynamics and
731 sedimentary development of the Dutch Wadden Sea with emphasis on the Frisian inlet.
732 Geologica ultraiectina, Mededelingen van de Faculteit Aardwetenschappen Universiteit
733 Utrecht no 126. 455pp.

734 Palmer, D.W., 1994. Growth of the razor clam *Ensis directus*, an alien species in the Wash on the east
735 coast of England. *J. Mar. Biol. Ass. U.K.* 84:1074-1076.

736 RIKZ, 2002. Noordzee-atlas voor zwevend stof op basis van satellietbeelden in 2000. eds:
737 Pasterkamp, R., van Drunen, M., Uitgave Min. Verkeer en Waterstaat, RIKZ/IT/2002.102, 33pp.

738 RWS, 2014. Programma Kustlijnzorg 2012-2015. Memo, Ministerie van Verkeer en Waterstaat, 39pp.

739 Severijns, N., 2002. Verspreiding van de Amerikaanse zwaardschede *Ensis directus* (Conrad, 1843) in
740 Europa 23 jaar na de introductie: opmerkelijke opmars van een immigrant. *Gloria Maris* 40 (4-
741 5), 63-111.

742 Trueman, E.R., 1967. The dynamics of burrowing in *Ensis* (Bivalvia). *Proc. R. Soc. Lond. B.* 166, 459-
743 476.

744 Tulp, I., Craeymeersch, J., Leopold, M. F., van Damme, C., Fey, F., Verdaat, H., 2010. The role of the
745 invasive bivalve *Ensis directus* as food source for fish and birds in the Dutch coastal zone.
746 *Estuar. Coast. Shelf Sci.*, 90, 116-128.

747 van der Heide, T., Tielens E., van der Zee, E.M., Weerman, E.J., Holthuijsen, S., Erikson, B.K., Piersma,
748 T., van de Koppel, J., Olf, H., 2014. Predation and habitat modification synergistically interact
749 to control bivalve recruitment on intertidal mudflats. *Biol. Conserv.*, 172, 163-169.

750 van der Hout, C.M., Gerkema, T., Nauw, J.J., Ridderinkhof, H., 2015. Observations of a narrow zone
751 of high suspended particulate matter (SPM) concentrations along the Dutch coast. *Cont. Shelf*
752 *Res.* 95, 27-38.

753 van der Hout, C.M., R. Witbaard, M.J.N. Bergman, G.C.A. Duineveld, M.J.C. Rozemeijer, T. Gerkema
754 (submitted). The dynamics of suspended particulate matter (SPM) and chlorophyll-a from
755 intratidal to annual time scales in a coastal turbidity maximum. *Neth. J. Sea Res. Special*
756 *volume North Sea.*

757 Von Cosel, R., Dörjes, J., Mühlenhardt-Siegel, U., 1982. Die amerikanische Schwertmuschel *Ensis*
758 *directus* (Conrad) in der Deutschen Bucht. I. Zoogeographie und taxonomie im vergleich mit
759 den einheimischen Schwertmuschel-Arten. *Senckenb. Marit.* 14, 147-173.

760 Widdows, J., Brinsley, M.D., Salkfield, P.N., Elliot, M., 1998. Use of annular flumes to determine the
761 influence of current velocity and bivalves on material flux at the sediment-water interface.
762 Estuaries 21 (4a), 552-559.

763 Willows, R.I., Widdows, J., Wood, R.G., 1998. Influence of an infaunal bivalve on the erosion of an
764 intertidal cohesive sediment: A flume and modelling study. Limnol. Oceanogr. 43(6), 1332-
765 1343.

766 Winter, A.G., Robin, V., Deits, L.H., Hosoi, A.E., 2012. Localized fluidization burrowing mechanics of
767 *Ensis directus*. J. Exp. Biol., 215, 2072-2080.

768 Witbaard, R., Duineveld, G.C.A., Bergman, M., 2001. The effect of tidal resuspension on benthic food
769 quality in the southern North Sea. Senckenb. Marit. 31(2), 225-234.

770 Witbaard, R., Duineveld, G.C.A., Bergman, M.J.N., 2013. The final report on the growth and dynamics
771 of *Ensis directus* in the near coastal zone off Egmond, in relation to environmental conditions.
772 NIOZ report 2013-2, 78pp.

773 Witbaard, R., Duineveld, G.C.A., Bergman, M.J.N., Witte, H.IJ., Groot, L., Rozemeijer, M.J.C., 2015.
774 The growth and dynamics of *Ensis directus* in the near-shore Dutch coastal zone of the North
775 Sea. J. Sea. Res. 95; 95-105.

776 Wolf, P., Meininger, P.L., 2004. Zeeën van zee-eenden bij de Brouwersdam. Nieuwsbrief NZG 5(2), 1-
777 2.

778 Wood, S.N., 2006. Generalized additive Models: An introduction with R. Chapman and Hall/CRC
779 press.

780 Zhou, Y., Zhang, S., Liu, Y., Yang, H., 2014. Biologically induced deposition of fine suspended particles
781 by filter-feeding bivalves in land-based industrial marine aquaculture wastewater. PLoS ONE
782 9(9), e107798. doi:10:1371/journal.pone.0107798.